

Thermal Plasma Processing
– Syntheses of Diamond and β'' -Alumina –

Osamu Fukumasa and Satoshi Sakiyama

*Department of Electrical and Electronic Engineering,
Faculty of Engineering, Yamaguchi University,
2-16-1 Tokiwadai, Ube 755-8611, Japan*

Abstract

Thermal plasma processing using a plasma jet with high speed and high heat capacity under reduced pressure (≤ 100 Torr) is one of the most promising methods for synthesizing new materials. We have newly developed a thermal plasma reactor composed of a forced constricted type plasma jet generator with a feed ring, and confirmed that this reactor generates stable plasma jets with a high heat capacity under various operating conditions. In this paper, to realize the large area deposition at a high rate, synthesis of diamond films from gas mixtures of CH_4 and H_2 is studied. Synthesis of β'' -alumina, thermoelectric materials for the alkali metal thermoelectric converter (AMTEC), from powder mixtures is also discussed.

Key words: thermal plasma processing, plasma jet, synthesis of new ceramics, diamond films, β'' -alumina

1. Introduction

Thermal plasma processing using a plasma jet with high speed and high heat capacity under reduced pressure (≤ 100 Torr) is one of the most promising methods for synthesizing new materials. To this end, we have developed a thermal plasma reactor [1] composed of a forced constricted type plasma jet generator with a feed ring, and confirmed that this reactor generates stable plasma jets with a high heat capacity under various operating conditions [2, 3]. So far, we have carried out a performance test of the reactor in the production of ultrafine particles [2, 3] and newceramics [4] and spray coatings of refractory materials [5], as well as in the synthesis of diamonds [6-8]. The typical deposition rate of spray coating with this system is about 5 $\mu\text{m/s}$ and that of diamond films is 5-6 $\mu\text{m/min}$. These deposition rates are higher than those of other methods by two or three orders of magnitude.

The alkali metal thermoelectric converter (AMTEC), which utilizes sodium ions which conduct β'' -alumina solid electrolyte, is a device that directly converts heat energy to electric energy [9,10]. In general, it is necessary to reduce the thickness of the β'' -alumina layer to improve the generating power densities. According to our recent experimental results [5], the characteristics of thin films prepared by plasma spraying depends strongly on the operating pressure and dense films without pores are obtained under a low pressure. We expect that β'' -alumina would be synthesized from powder mixtures and dense and thin β'' -alumina coatings would be prepared successively by low-pressure plasma spraying. On the other hand, a porous molybdenum electrode is expected to be prepared under atmospheric pressure.

In this paper, the diamond synthesis from gas mixtures, and synthesis of β'' -alumina from powder mixtures are presented. For diamond synthesis [6, 8], we will discuss the correlation between the optical emission spectra for the plasma jet and the deposited diamond, with a view toward increasing the deposition area of the diamond film. For β'' -alumina synthesis [4], we will discuss the relationship between the temperature of the plasma jet and the synthesis of β'' -alumina films.

2. Experimental Set Up

A schematic drawing of the plasma reactor system [4-8] used in the present work is shown

in Fig.1. The system consists of the forced constricted type (FC-type) plasma jet generator (the nozzle anode made of copper with 5 mm diameter, the insulated constrictor nozzle made of copper with 5 mm diameter, and rod cathode made of 2%Th-W), the feed ring (FR) (5mm diameter) and the vacuum vessel (160 mm diameter by 500 mm length).

Experiments are performed under continuous pumping and flowing of argon gas. The plasma jet is produced by DC arc discharge. As the insulated constrictor nozzle peculiar to this generator always fixes the arc length and the nozzle wall strongly constricts the arc with working gas, the plasma jet is kept very stable and has high power under various experimental conditions. For diamond synthesis [6-8], material gas (methane and hydrogen mixture) is radially injected into the plasma jet through the feed ring. Diamond is synthesized on the molybdenum or silicon substrate (16 mm diameter) held on the water cooled substrate holder which is set against the plasma jet. The substrate is scratched by Al₂O₃ particles with mean diameter of 20μm for 120 min. before the experiment. The substrate temperature is estimated using a pyrometer. For β"-alumina synthesis[4], powder materials were injected into the plasma with carrier gas through two capillary feeding ports of the FR. For the synthesis of β"-alumina, powder mixtures of α-Al₂O₃, Na₂CO₃ and MgO were used.

Experiments are made under the following conditions: working gas (Ar) flow rate is 20l/min., jet power (W_j) is 3 - 6 kW, pressure in reaction chamber (P_t) is 5-760 Torr, methane gas flow rate is 0.1-1 l/min., hydrogen gas flow rate is 5 l/min., powder feed rate is 0.5 g/min., the distance from the feed ring exit to substrate (L) is 25-110 mm.

3. Experimental Results and Discussion

3.1. Behavior of plasma jet versus vessel pressure

Fig. 2 shows the photographs of the plasma jet at $P_t = 760, 100$ and 5 Torr. Under low pressure, the plasma jet expands and its diameter increases to about 50 mm at 5 Torr. Namely, with decreasing P_t , plasma jet increases in its size of both the axial and radial directions. Corresponding to this, high temperature region and high velocity region expand. For example, the volume at 100 Torr where the temperature of the plasma jet is higher than the melting point of alumina is as about 4.4 times large as that at 760 Torr, and velocity of the plasma jet at $L = 50$ mm increase from about 100 m/s to 530 m/s [2]. With increasing W_j , as

is shown in Fig.3, high temperature and high velocity regions further expand in the downstream region.

Therefore, we can control the volume and velocity of the plasma jet by varying P_t . In order to realize the large area deposition, we have studied the effect of P_t on diamond synthesis [6]. In plasma spraying [5], it is also important that injected particles are fully melted and collided to the substrate with high speed. Therefore, by using plasma jet under low pressure, it is expected to obtain dense coating and to realize the plasma processing with high rate and large area deposition.

3.2. Synthesis of diamond

In diamond synthesis using the thermal plasma jet, the deposited particles and films strongly depend on the ratio of methane gas flow rate to hydrogen gas flow rate (CH_4/H_2), the distance from the feed ring exit to the substrate (L), and substrate temperature (T_s). Fig. 4 shows the relationship between morphology of the deposited particles and CH_4/H_2 where T_s is kept constant at $1050\pm 50^\circ\text{C}$. Deposition time is 10 min. Three types of particles are prepared: polyhedral particles (type A), spherical particles which involve the (100) crystal plane (type B) and only spherical particles (type C). According to the results of Raman spectroscopy and X-ray diffraction (not shown here), the particles of type A and type B are diamond, but type C is not. Furthermore, the diamond of type A is purer than that of type B.

In order to synthesize a diamond film with high quality and high deposition rate, we must choose the experimental conditions such that particles of type A are deposited. Based on the results shown in Fig.4, we synthesize diamond film keeping $\text{CH}_4/\text{H}_2 = 3\%$, and study the effect of vessel pressure on diamond synthesis.

Fig. 5 shows the scanning electron microscope (SEM) photographs of the diamond films obtained under two different pressures. The size of crystals which compose the film, is smaller under low pressure than that under atmospheric pressure. Therefore, the surface of the film becomes flatter with decreasing P_t . From those SEM photographs, we estimate the thickness of the films and deposition area. The thickness of the film at the center gradually decreases with decreasing P_t . On the other hand, the deposition area increases markedly with decreasing P_t . When $P_t = 5$ Torr, the substrate (16 mm diameter) is fully covered by the diamond film.

For clarification of the relationship between the morphology of the deposited particles shown in Fig.4 and the chemical species in the plasma jet, emission spectra were measured. The spectra of Balmer series hydrogen (H_α , H_β and H_γ), the hydrocarbon radical CH and dicarbon, C_2 , have attracted special interest, because they seem to be related to the morphology of the deposited particles.

We have obtained the two-dimensional distributions of the optical emission spectra (i.e. H_α , CH and C_2) from the plasma jet, which is converted from the measured line intensity by means of Abel inversion. The spectral intensity decreases with increasing distance from the feed ring exit, but increases again in the vicinity of the substrate. The diameter of the plasma flame also decreases slightly with increasing distance from the feed ring exit and then rapidly increases in front of the substrate. Namely, plasma flow stagnates in front of the substrate. We consider this stagnation of the plasma flow to be strongly correlated with the quality of the deposited particles and the deposition area.

We compare the radial distribution of H_α (656.2 nm) with that of CH (431.4nm) at 1 mm above the substrate for P_t of 7 and 20 Torr where methane gas flow rate $Q(CH_4)$ is 0.15 l/min. Under the conditions of the high quality diamond (type A) particle deposition, the H_α line intensity is the highest and the intensities of the CH and the C_2 spectra are the lowest. On the other hand, under the conditions non-diamond particle (type C) deposition, the H_α intensity is the lowest and the intensities of the CH and the C_2 spectra are the highest. From these results, we can conclude that diamond is synthesized under conditions of a high H atom density and low CH and C_2 molecular densities.

The intensity ratios among the spectra seem to be important in terms of the quality of the deposited diamond particles. Fig. 6 shows the radial distributions of the intensity ratio of CH to H_α (CH/H_α). These distributions are calculated by division of the intensity of the CH spectrum by that of the H_α spectrum. Apparently, diamond particles (type A and type B) are synthesized under the condition that CH/H_α is rather small. With increasing CH/H_α , the deposited particles vary from diamond to graphite. Therefore, the radial distributions of CH/H_α were compared with the area of the diamond films obtained. As shown in Fig.6, when $P_t = 20$ and 7 Torr, corresponding to this, CH/H_α remains nearly constant from the substrate center to radius $r = 8$ and 12 mm, respectively, and the diamond film obtained under

the same conditions is about 7 and 12 mm. This diamond film radius is almost equal the radius (R_{CH/H_α}) at which CH/H_α remains nearly constant. For various operating conditions, the radius of the diamond film is also found to be nearly equal to R_{CH/H_α} . That is to say, diamond is synthesized in the region where CH/H_α has a certain small constant value. In Fig.6, the parameter is P_t . For the relationship between the radius of diamond film and R_{CH/H_α} , the same tendency is observed when the parameters are the distance from the feed ring exit to the substrate and methane gas flow rate [7, 8]. In conclusion, the deposition area of the diamond film can be estimated by monitoring CH/H_α .

Furthermore, we investigated the possibility of changing CH/H_α or modifying the quality of the deposited diamond by injection of additional hydrogen into the plasma jet. We fed the additional hydrogen into the plasma fringe near the substrate using a copper tube. With increasing additional hydrogen flow rate, CH/H_α increases at the plasma fringe and, at the same time, the quality of the deposited diamond film deteriorates. Therefore, we have reconfirmed that the intensity ratio CH/H_α is promising parameter for monitoring of diamond synthesis. It may be possible to increase the area of diamond synthesis by decreasing P_t and optimizing the conditions for the additional hydrogen injection.

3.3. Synthesis of β'' -alumina

The synthesis of β'' -alumina was attempted using powder mixtures of α - Al_2O_3 , Na_2CO_3 and MgO. As β -alumina can be successfully synthesized from mixtures of α - Al_2O_3 and Na_2CO_3 and the optimum percentage composition of Na_2CO_3 ranges from 10 to 20 percent, we tested the synthesis of β'' -alumina using powder mixtures to which MgO was added as the third material[11]. The effect of MgO on β'' -alumina synthesis is studied as a function of the percentage composition of MgO, because MgO plays an important role in stabilizing β'' -alumina chemically. When the percentage composition of the MgO is increased, peaks of β'' -alumina appear and their intensities increase. When the percentage composition of the MgO is higher than 15%, however, the intensities conversely decrease [4,11]. It suggests that β'' -alumina is synthesized from powder mixtures of α - Al_2O_3 , Na_2CO_3 and MgO, and there is an optimum percentage composition of MgO for synthesizing β'' -alumina.

As far as we know, β'' -alumina films synthesized here are the first ones prepared by thermal plasma processing, although β -alumina is included. Also, there are some peaks of

raw powder materials, i.e., peaks of α - Al_2O_3 , Na_2CO_3 and MgO , in the X-ray diffraction patterns of the prepared films. To obtain a high thermoelectric conversion efficiency, pure β'' -alumina films must be synthesized. To optimize the processing conditions, we discuss the effects of the jet power W_j , the chamber pressure P_t and the distance L between the feed ring exit and the substrate on the synthesis of β and β'' -alumina films.

As shown in Fig.2, with decreasing chamber pressure P_t , the plasma jet increases in size in both axial and radial directions. Correspondingly, in Fig.3, the high-temperature region and the high-velocity region expand. Fig. 7 shows the axial distributions of the plasma jet temperature at two different pressures, 760 Torr and 100 Torr. As is clearly shown, with increasing W_j or decreasing P_t , the high-temperature region shifts to the downstream region.

Fig. 8 shows the X-ray diffraction patterns of the synthesized films as a function of L at $P_t = 100$ Torr. In the downstream region where L is greater than 70 mm, a small peak of β'' -alumina is observed among the many peaks of the raw powder materials. On the other hand, in the upstream region where L is less than 60 mm, many β'' -alumina peaks appear distinctly and their intensities increase markedly with decreasing L . At $L = 50$ mm, β'' -alumina peaks become dominant, although small β -alumina and small MgO peaks are observed, but not Mo peaks, i.e., the substrate material. It is suggested that pure β'' -alumina films are well synthesized in the upstream region of the plasma jet, i.e., the high-temperature region of the plasma jet. According to film analysis by EPMA, the ratio of Na to Al in the prepared films (at $L = 50$ mm) ranges from 1/4.7 to 1/6. This value is nearly the same as that of β'' -alumina films prepared ideally, i.e. 1/5-1/7.

On the other hand, under atmospheric pressure, we have confirmed the same tendency that β and β'' -alumina films are well synthesized with decreasing L . The optimum value of L is less than 30 mm. Taking into account the results shown in Figs.7 and 8 and the discussion described above, there should be a strong correlation between the jet temperature and the synthesis of β'' -alumina films. Though the axial jet temperature is nonuniform at each gas pressure (i.e, 100 and 760 Torr), the temperature in the region where β'' -alumina films are well synthesized is nearly the same regardless of pressure. Namely, the value is nearly equal to 2400°C , regardless of P_t .

Fig. 9 shows typical SEM images of the deposited film at $L = 80$ mm and 40 mm under P_t

= 100 Torr. According to the X-ray diffraction patterns shown in Fig.8, β and β'' -alumina are synthesized more successfully in Fig.9 (b). The film in Fig.9 (a) is composed of particles with diameter less than $10\mu\text{m}$, which are not well melted, and the film is porous. On the other hand, the film in Fig.9 (b) is dense as the deposited powders are well melted.

The melting points of Na_2CO_3 (852°C) and MgO (2800°C) are quite different. For β'' -alumina synthesis, more sodium ions should be included in the prepared films than in β -alumina films. Therefore, at least MgO (i.e., the stabilizer of sodium ions) should be well melted in front of the substrate. Thus, β'' -alumina is well synthesized in a high-temperature region (above 2400°C) of the plasma jet, and the optimum percentage composition of Na_2CO_3 also depends on the plasma jet temperature (or L and W_j)[4].

The performance characteristics of the AMTEC strongly depend on two physical constants of the β'' -alumina films, i.e., the thermal and electrical conductivities. In the preparation of β'' -alumina, W_j , L and the percentage composition of powder mixtures have been found to be the key parameters, which are correlated with the plasma jet temperature and heat transfer from plasmas to particles. Optimization of the processing conditions where β'' -alumina films with required physical constants are prepared is studied in the future.

4. Conclusions

In this paper, syntheses of diamond films and β'' -alumina films by using plasma jets under low-pressure, is studied. In case of diamond, the morphology of deposited particles strongly depends on the ratio of methane gas flow rate to hydrogen gas flow rate, CH_4/H_2 , and on the distance from the feed ring exit to the substrate, L . To clarify the relationship between the morphology of the prepared particles and the chemical species in the plasma jet, emission spectra from the plasma jet have been studied. The spectra of the Balmer series of hydrogen, hydrocarbons and dicarbon have attracted special interest. Among these spectra, the spectral intensity ratio of CH to H_α at 1 mm above the substrate has a strong correlation with the quality of synthesized diamond and its deposition area. In case of thermoelectric materials (β'' -alumina) for the alkali metal thermoelectric converter (AMTEC), thin films of β'' -alumina are successfully synthesized for the first time from powder mixtures of $\alpha\text{-Al}_2\text{O}_3$, Na_2CO_3 and MgO not only under atmospheric pressure but also under low pressure. The

powder mixing ratio, jet power and substrate position strongly affect the synthesis of β "-alumina, which is found to be correlated with jet temperature.

Acknowledgement

A part of this work is supported by a Grant-in-Aid for Developmental Scientific Research from The Japanese Ministry of Education, Science, Sports and Culture. This work is also supported by a Grant-in-Aid for Regional Consortium Project from New Energy and Industrial Technology Development Organization (NEDO), Japan.

References

- [1] S. Saeki, O. Fukumasa and K. Osaki, *Proc. 8th Int. Symp. Plasma Chemistry* **3** (1987) 1989.
- [2] O. Fukumasa and S. Sakiyama, *Trans. IEE Jpn.* **112A** (1992) 269. (in Japanese)
- [3] S. Sakiyama, T. Hirabaru and O. Fukumasa, *Rev. Sci. Instrum.* **63** (1992) 2408.
- [4] O. Fukumasa and S. Sakiyama and H. Esaki, *Jpn. J. Appl. Phys.* **38** (1999) 4571.
- [5] O. Fukumasa, S. Sakiyama and K. Osaki, *Proc. The Japan-China Bilateral Symp. Advanced Materials Engineering* (1999) p.58.
- [6] S. Sakiyama, O. Fukumasa and K. Aoki, *Jpn. J. Appl. Phys.* **33** (1994) 4409.
- [7] S. Sakiyama, O. Fukumasa, T. Murakami and T. Kobayashi, *Jpn. J. Appl. Phys.* **36** (1997) 5003.
- [8] S. Sakiyama and O. Fukumasa, *J. Jpn. Inst. Metals*, **63** (1999) 55. (in Japanese)
- [9] T. Cole: *Science* **221** (1983) 915.
- [10] T. Masuda: *Ceramics* **25** (1990) 609. (in Japanese)
- [11] O. Fukumasa, S. Sakiyama, Y. Shirai and K. Hatano, *Proc. 13th Symp. Plasma Processing* (1996), p.157.

Figure Captions

Fig.1. Schematic diagram of the plasma jet reactor system.

Fig.2. Photographs of the plasma jet for three different pressures. Experimental conditions are as follows: Jet power $W_j = 3$ kW, Working gas flow rate Q (Ar) = 20 l/min, and $CH_4/H_2 = 3\%$

Fig.3. Temperature and velocity fields of the plasma jet for two different pressures.

Fig.4. Relationship between morphology of the particles and flow rate CH_4/H_2 . Type A, type B and type C indicate polyhedral particles, spherical particles which involve (100) crystal plane and only spherical shape particles, respectively. Experimental conditions are as follows: $P_t = 55$ Torr, $W_j = 3$ kW, and substrate temperature $T_s = 1050 \pm 50^\circ C$.

Fig.5. SEM photographs of the diamond films obtained under two different pressures. Experimental conditions are as follows: $W_j = 3$ kW, $CH_4/H_2 = 3\%$, $T_s = 1050 \pm 50^\circ C$ and deposition time = 10 min.

Fig.6. The radial distributions of the intensity ratio of CH to H_α (CH/H_α) for two different pressures. They correspond to the radial distributions of H_α (656.2 nm) and CH (431.4 nm) at 1 mm above the substrate for P_t of 7 and 20 Torr where methane gas flow rates $Q(CH_4)$ is 0.15 l/min. This flow rate corresponds to deposition of type A diamond.

Fig.7. Axial distribution of the plasma jet temperature in the downstream region for two different pressures $P_t = 100$ and 760 Torr.

Fig.8. X-ray diffraction patterns of the thin films as a function of L . Experimental conditions are as follows: $W_j = 3$ kW, $P_t = 100$ Torr and powder mixtures are $\alpha-Al_2O_3$ (77 %) + Na_2CO_3 (14 %) + MgO (9 %).

Fig.9. SEM images of the prepared thin films. Experimental conditions are as the same as ones in Fig.8.

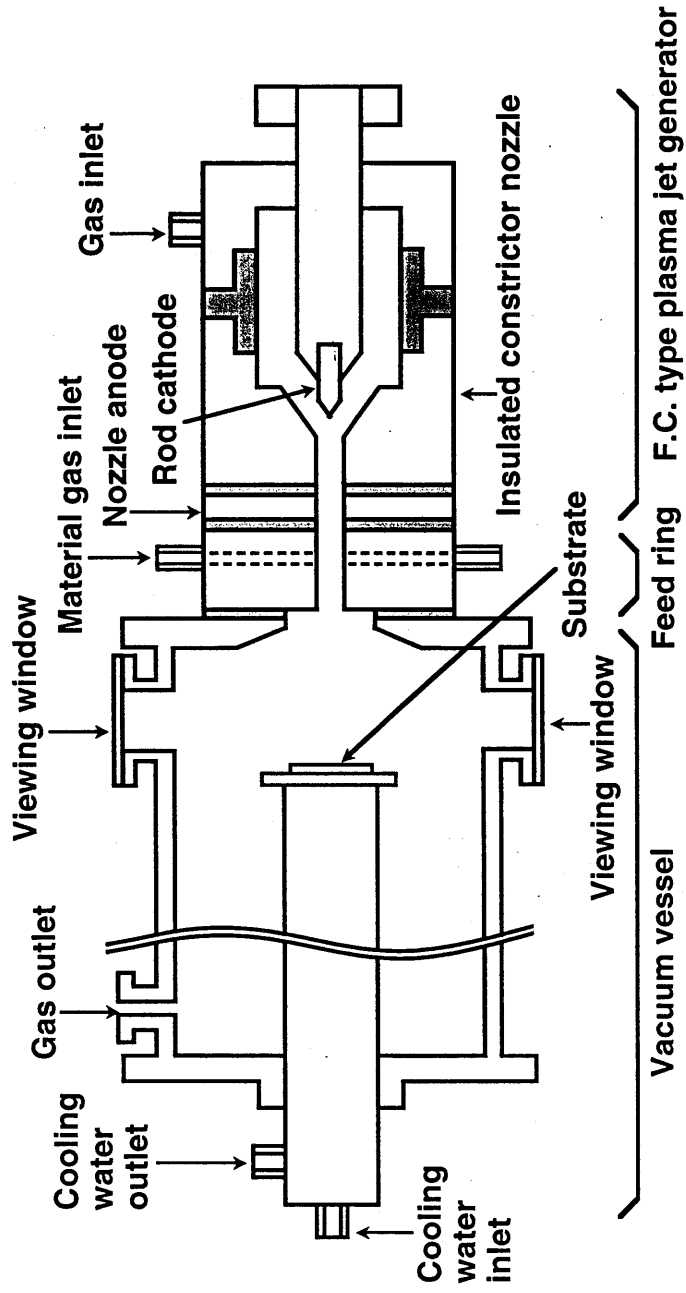
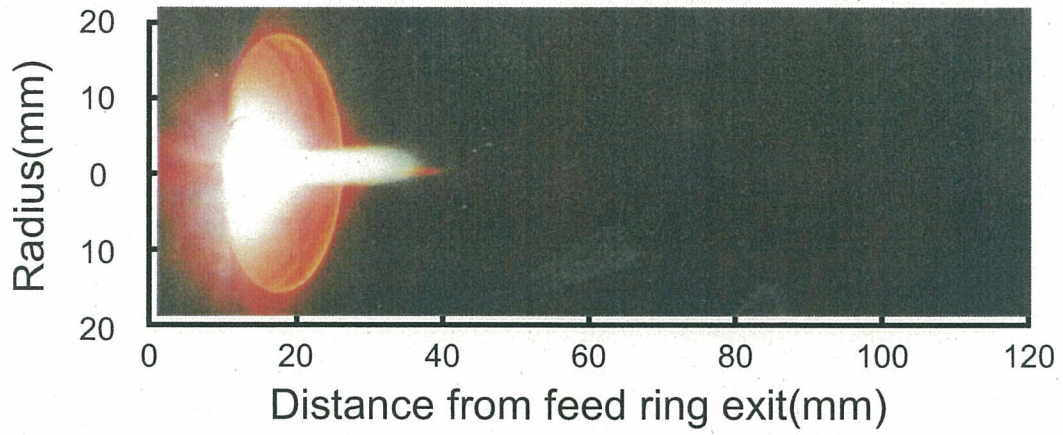
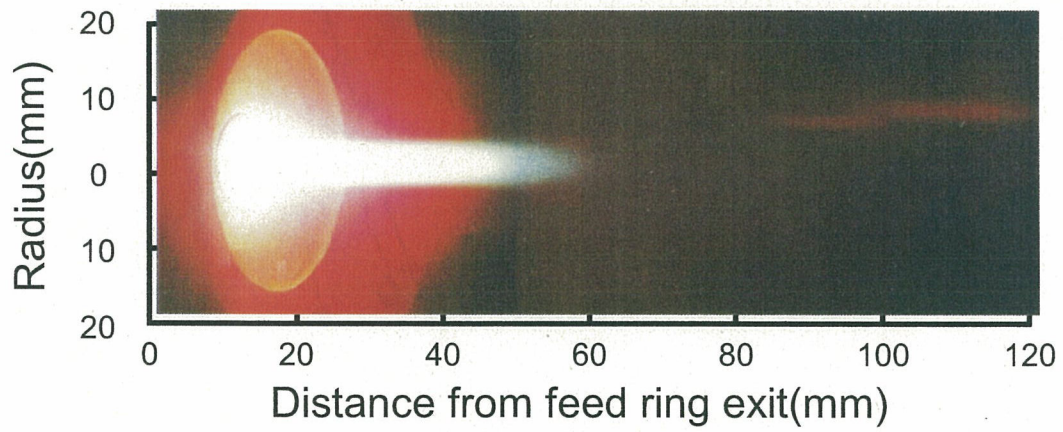


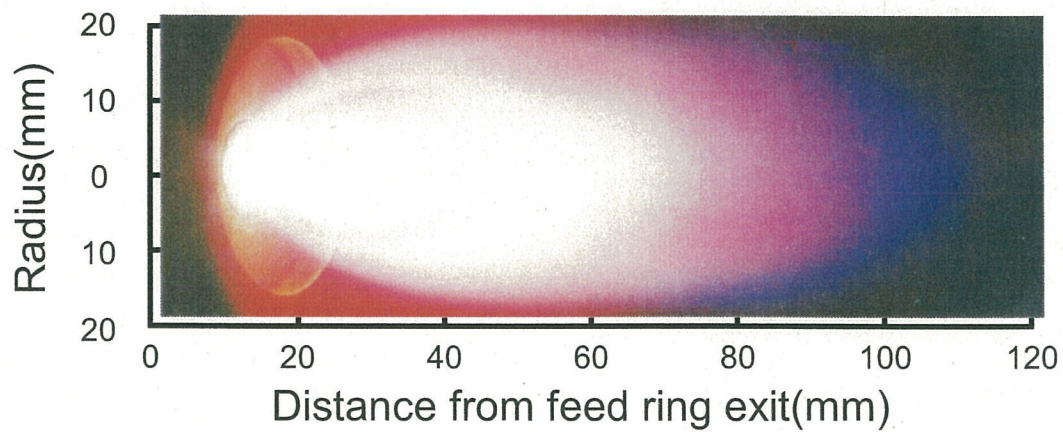
Fig.1 O. Fukumasa



(a) Pt = 760 Torr

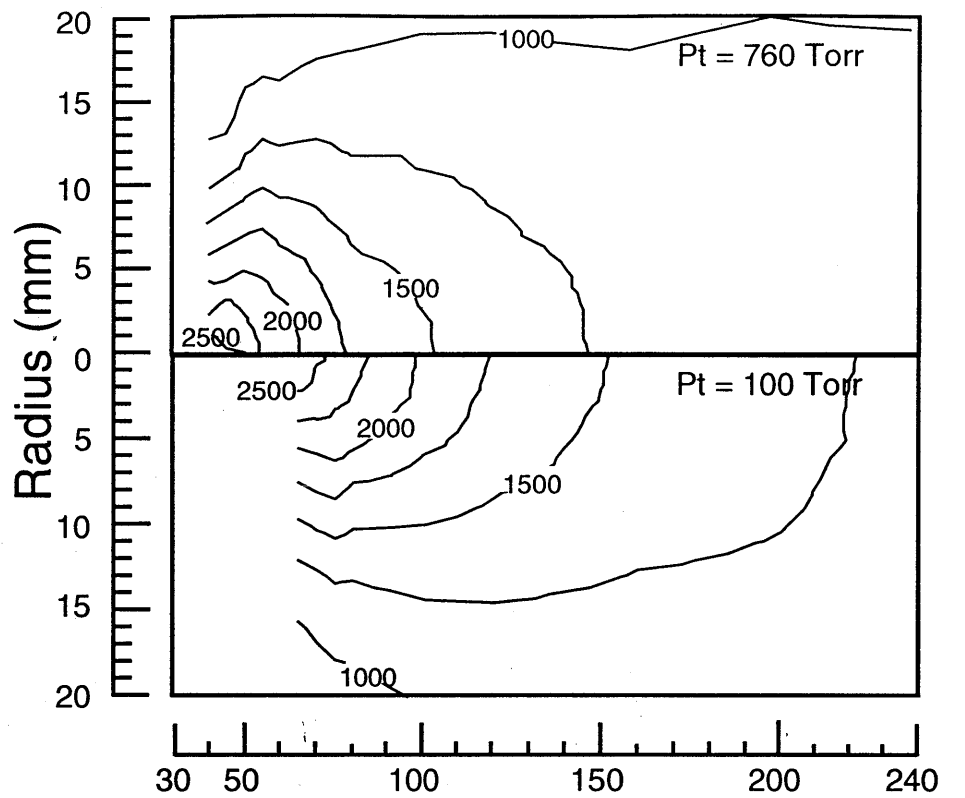


(b) Pt = 100 Torr

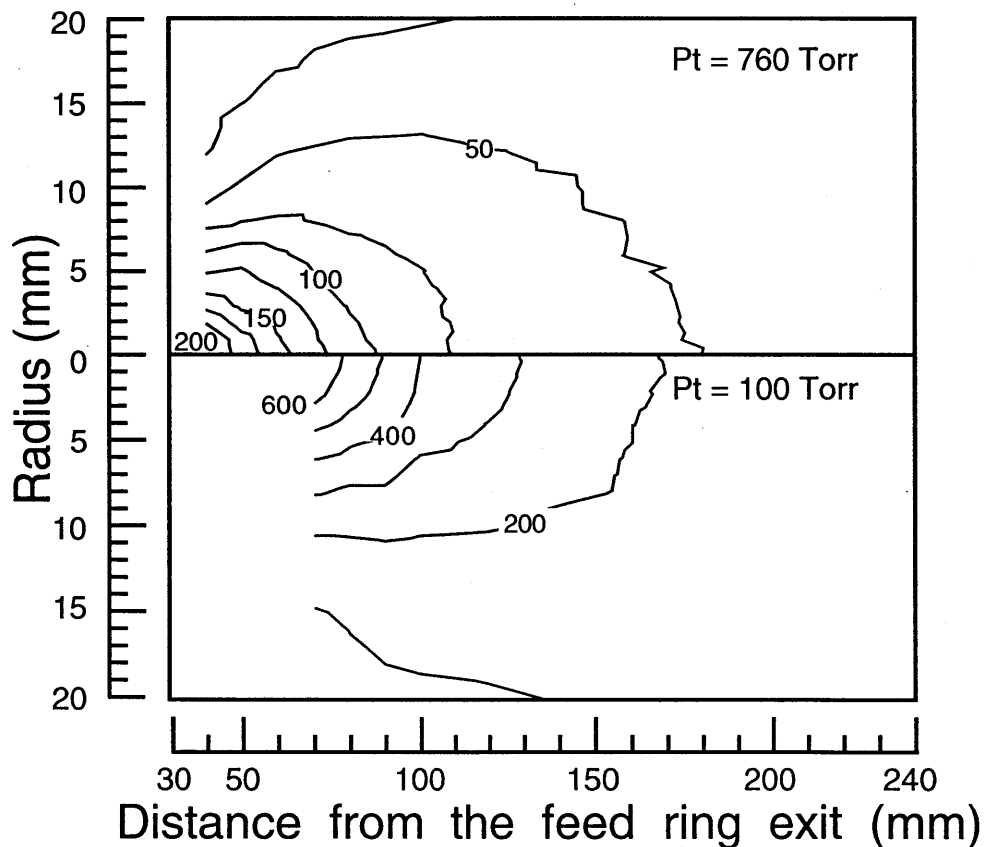


(c) Pt = 3 Torr

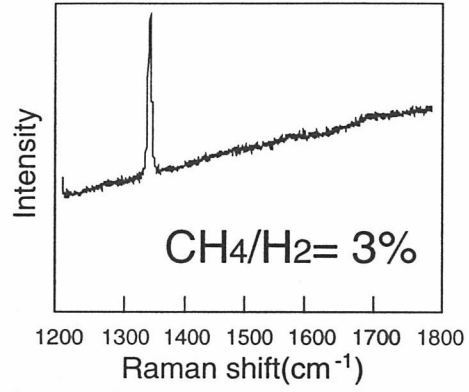
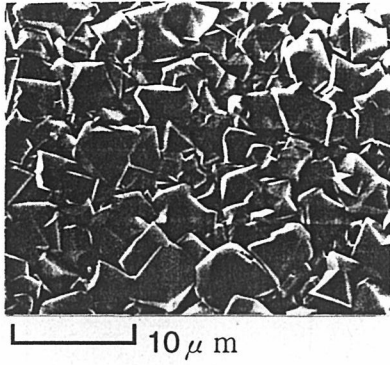
Fig. 2 O. Fukumasa



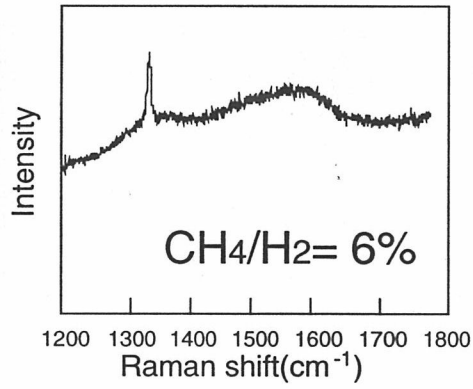
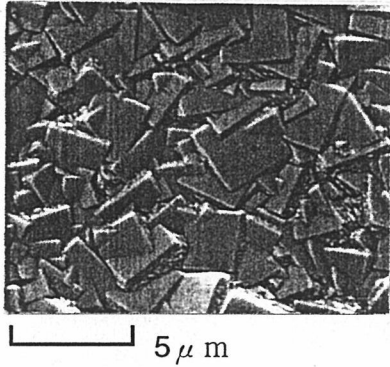
Distance from the feed ring exit (mm)
 (a) Temperature (K)



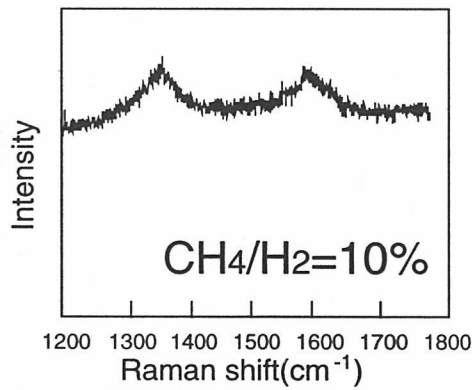
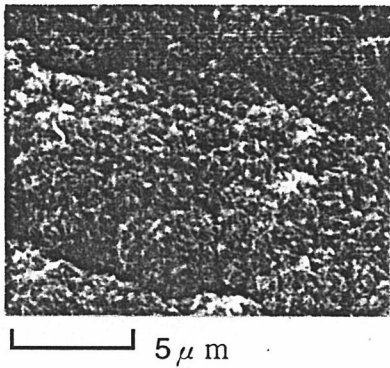
Distance from the feed ring exit (mm)
 (b) Velocity (m/s)



(a) Type A



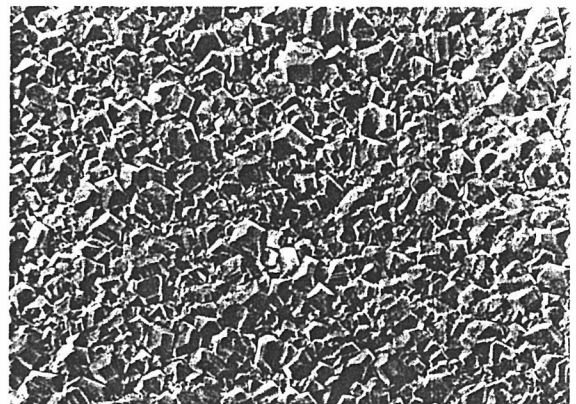
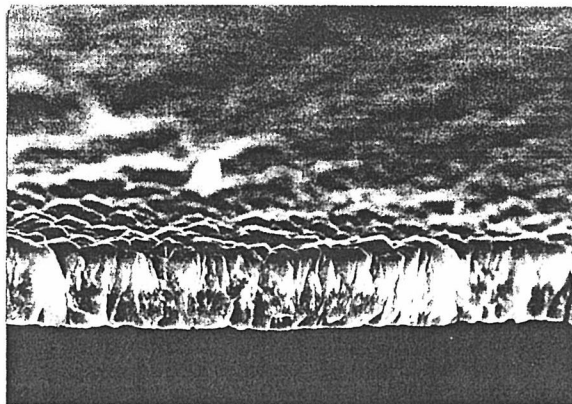
(b) Type B



(c) Type C



(a) Pt = 760 Torr



(b) Pt = 5 Torr

Fig 5 O. Fukumasa

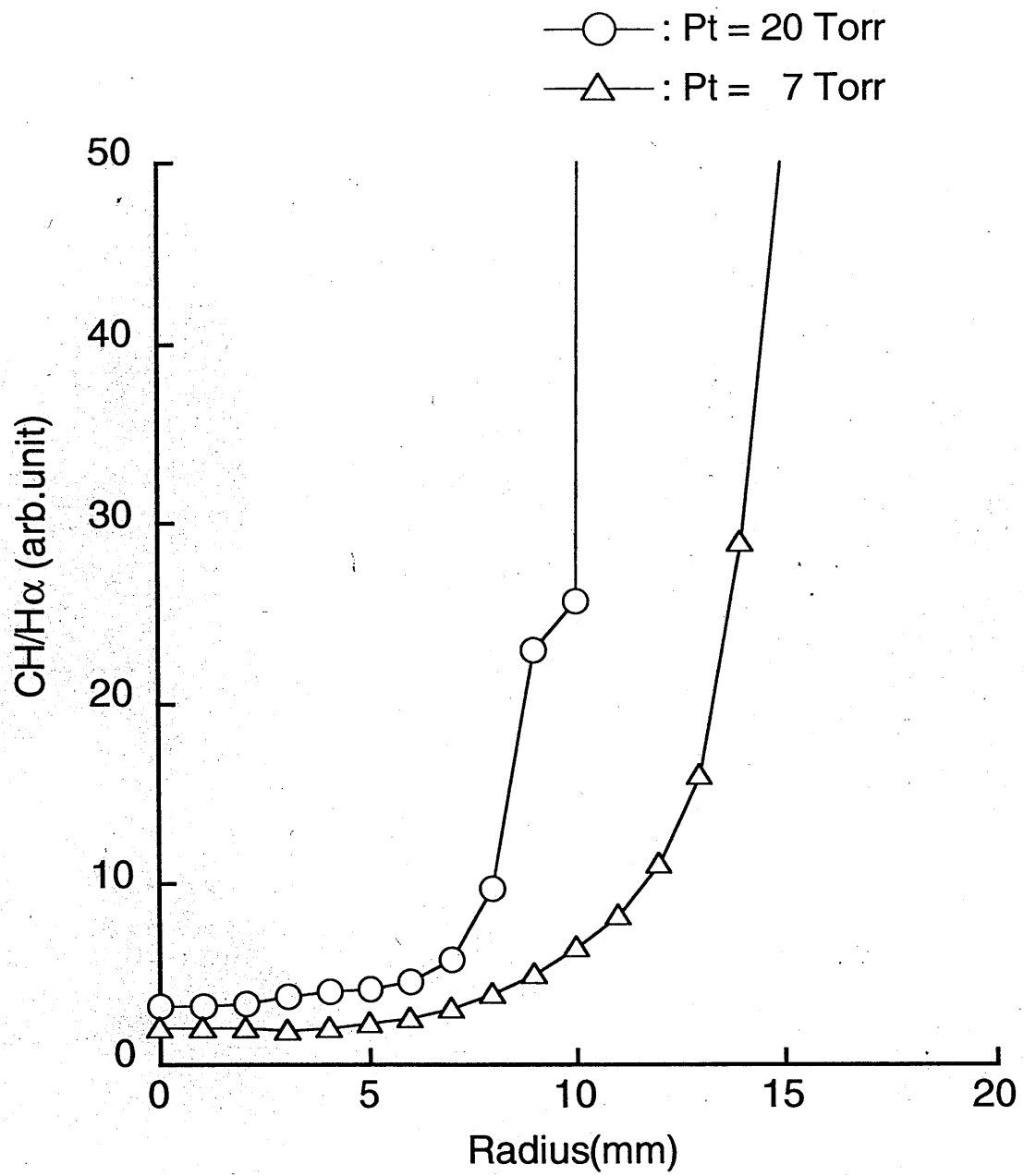


Fig. 6 O. Fukumasa

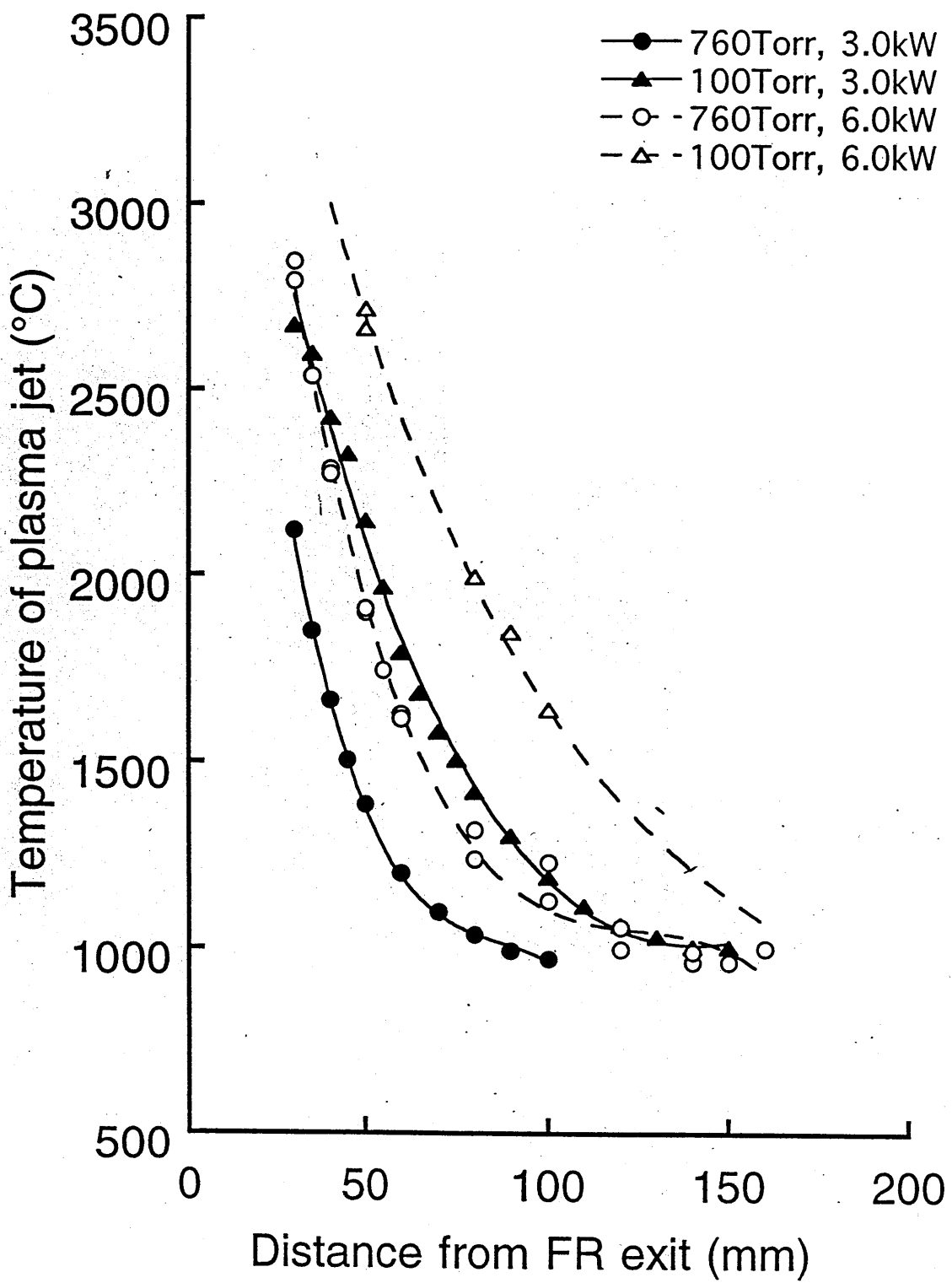


Fig. 7 O. Fukumasa

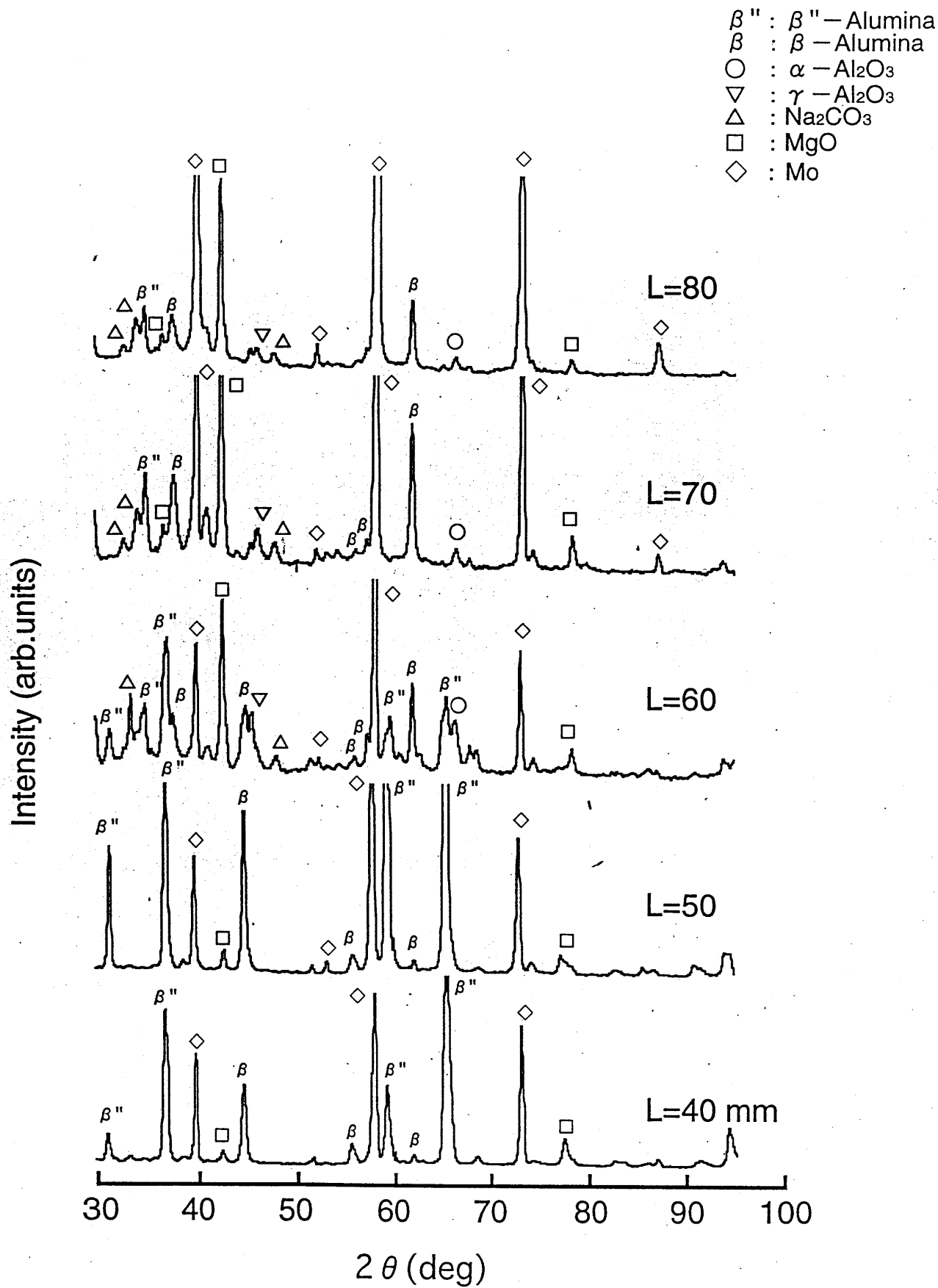
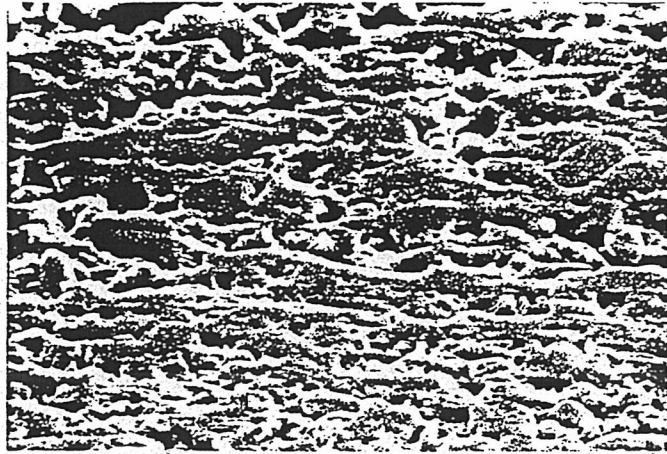


Fig. 8 O. Fukumasa

Cross-sectional view



50 μ m

(a) L=80 mm



50 μ m

(b) L=40 mm

Fig. 9 O. Fukumasa